In Vitro Ligation of Oligodeoxynucleotides Containing C8-Oxidized Purine Lesions Using Bacteriophage T4 DNA Ligase†

Xiaobei Zhao, James G. Muller, Mohan Halasyam, Sheila S. David, and Cynthia J. Burrows*

Department of Chemistry, University of Utah, 315 South 1400 East, Salt Lake City, Utah 84112-0850

Received October 25, 2006; Revised Manuscript Received January 30, 2007

ABSTRACT: Ligases conduct the final stage of repair of DNA damage by sealing a single-stranded nick after excision of damaged nucleotides and reinsertion of correct nucleotides. Depending upon the circumstances and the success of the repair process, lesions may remain at the ligation site, either in the template or at the oligomer termini to be joined. Ligation experiments using bacteriophage T4 DNA ligase were carried out with purine lesions in four positions surrounding the nick site in a total of 96 different duplexes. The oxidized lesion 8-oxo-7,8-dihydroguanosine (OG) showed, as expected, that the enzyme is most sensitive to lesions on the 3′ end of the nick compared to the 5′ end and to lesions located in the intact template strand. In general, substrates containing the OG·A mismatch were more readily ligated than those with the OG·C mismatch. Ligations of duplexes containing the OA·T base pair (OA = 8-oxo-7,8-dihydroadenosine) that could adopt an *anti*−*anti* conformation proceeded with high efficiencies. An OI·A mismatch-containing duplex (OI = 8-oxo-7,8-dihydroinosine) behaved like OG·A. Due to its low reduction potential, OG is readily oxidized to secondary oxidation products, such as the guanidinohydantoin (Gh) and spiroiminodihydantoin (Sp) nucleosides; these lesions also contain an oxo group at the original C8 position of the purine. Ligation of oligomers containing Gh and Sp occurred when opposite A and G, although the overall ligation efficiencies were much lower than those of most OG base pairs. Steady-state kinetic studies were carried out for representative examples of lesions in the template. K_m increased by 90−100-fold for OG·C-, OI·C-, OI·A-, and OA·T-containing duplexes compared to that of a G·C-containing duplex. Substrates containing Gh·A, Gh·G, Sp·A, and Sp·G base pairs exhibited K_m values 20−70-fold higher than that of the substrate containing a G·C base pair, while the K_m value for OG·A was 5 times lower than that for G·C.

Reactive oxygen species (ROS)[1] such as $O_2^{-\bullet}$, HO•, and H_2O_2 are continuously produced during normal metabolic processes, and their production is augmented by inflammation and exposure to certain agents (*1*, *2*). DNA is sensitive to ROS, and in vivo oxidative damage results in DNA strand breaks, base modifications, and DNA−protein cross-links (*1*). Unrepaired oxidative DNA damage can be mutagenic and is implicated in carcinogenesis, neurological disorders, and aging (*2*−*4*). Oxidation of guanine, the most easily oxidized nucleobase (*5*), can lead to the commonly observed lesion 8-oxo-7,8-dihydro-2′-deoxyguanosine (OG) which is regarded as a biomarker of oxidative DNA damage in the cell (*6*). OG is mutagenic in the absence of repair, leading to G → T transversions (*7*−*10*).

OG can be removed by the base excision repair (BER) pathway (*11*−*14*) involving glycosidic bond cleavage of the damaged base followed by excision of the remaining abasic (AP) site (*15*). A nucleotide is inserted by a DNA polymerase, and in a final stage, the nick is sealed by a DNA ligase (*16*−*20*). Although DNA repair of oxidized base lesions has been extensively investigated, only a few studies describing the effect of oxidized base lesions on DNA ligation, the last step of DNA repair, have appeared (*21*, *22*). Both human DNA ligases I (Ligl) and III are able to join an OG·A base pair more efficiently than an OG·C base pair when A or C is inserted at the 3′ end of the nick (*23*). Lig1 also joins Okazaki fragments and aids in long-patch base excision repair (*24*−*26*). The crystal structure of Lig1 complexed with an adenylated DNA intermediate was recently reported and aids in the understanding of its interaction with the DNA substrate at the catalytic core (*27*).

This study was designed with the aim of gaining an understanding of how oxidized purines located at different positions surrounding the nick site in the DNA duplex influence the ligation efficiency of bacteriophage T4 DNA ligase (EC 6.5.1.1). T4 DNA ligase is widely used as a tool in gene manipulation, and its low fidelity makes it a good starting point for studying DNA ligation. Ligases catalyze the formation of a phosphodiester bond between the 5′-phosphoryl and 3′-hydroxyl termini to close a nick in duplex DNA or RNA (*28*). T4 DNA ligase is purified from *Escherichia coli* and uses ATP as a cofactor in this process (*28*, *29*). The ligation mechanism involves three steps: (a)

†This work was supported by the National Cancer Institute (Grant CA090689).

* To whom correspondence should be addressed. Phone: (801) 585-7290. Fax: (801) 585-0024. E-mail: burrows@chem.utah.edu.

[1] Abbreviations: ROS, reactive oxygen species; OG, 8-oxo-7,8-dihydroguanine; Gh, 5-guanidinohydantoin; Sp, spiroiminodihydantoin; OI, 8-oxo-7,8-hypoxanthine; OA, 8-oxo-7,8-dihydroadenine; BER, base excision repair; PAGE, polyacrylamide gel electrophoresis; ESI-MS, electrospray ionization mass spectrometry; Ligl, human DNA ligase I; APE1, human apurinic endonuclease 1.

10.1021/bi062214k CCC: $37.00
Published on Web 02/27/2007

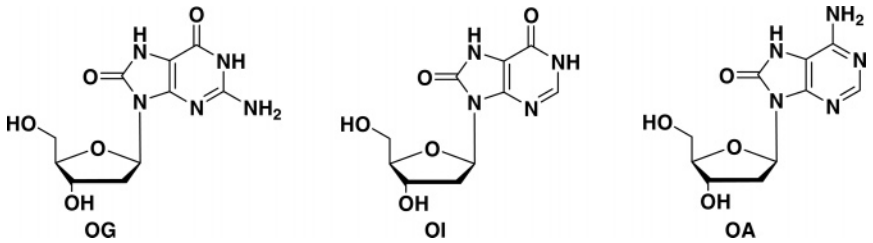

FIGURE 1: Structures of 8-oxo-7,8-dihydro-2′-deoxyguanosine (OG), 8-oxo-7,8-dihydro-2′-deoxyinosine (OI), and 8-oxo-7,8-dihydro-2′-deoxyadenosine (OA).

activation of the enzyme by adenylation (*30*), (b) formation of the intermediate by transfer of the AMP residue from the enzyme to the 5′-phosphate of the nicked DNA (*30*), and (c) sealing of the DNA by a transesterification reaction (*28*, *31*). The existence of clustered DNA damage (*32*−*35*) and the insertion of dOGMP during replication suggest the possibility that an oxidized lesion could appear near a nick site. Furthermore, the DNA repair enzyme MutY excises adenine opposite guanine or 8-oxoG during BER (*11*, *36*, *37*), and complete repair requires the further action of a polymerase for insertion of dCTP opposite OG, followed by ligation (*38*). In this case, the ligase would be required to seal the nick with an OG·C base pair at the junction. T4 DNA ligase is a low-fidelity enzyme, which allows it to seal various mismatches, particularly the G·T mismatch (*39*, *40*); however, mismatches at the duplex terminus are known to slow the ligation reaction (*41*). The efficiency of T4 DNA ligase in ligating two oligodeoxynucleotides greatly decreases when single-base pair mismatches appear on either side of the ligation junction (*42*, *43*). Previous studies reported that T4 DNA ligase is capable of ligating C·T and G·T mismatches on the 3′ end of the nick and can tolerate pyrimidine/pyrimidine mismatches better than purine-containing mismatches (*44*−*46*).

The purpose of this study was to investigate the ability of T4 DNA ligase to seal a nick that contains an oxidized base lesion at or near the ligation site. OG and other oxidized purines, such as 8-oxo-7,8-dihydroadenine (OA), occur frequently in mammalian cells (Figure 1) (*47*, *48*). A previous study showed that OA may contribute to carcinogenesis via the observation that it appears in human tumor tissue at an increased level (*49*). OA·T and OG·A base pairs with the oxidized lesion positioned at the 3′ end of the nick were reported to have a high ligation efficiency with T4 DNA ligase (*50*). 8-Oxo-7,8-inosine (OI) has a structure similar to that of OG but lacks the 2-amino group and serves as a structural probe (Figure 1). Both OG and OI have carbonyl groups at C6 and can base pair with A at a *syn*−*anti* conformation (*51*). OA, with an amino group at C6, preferentially pairs with T in an *anti*−*anti* conformation, although it can also mispair with G, leading to A → C transversions (*52*, *53*). The OA·C mismatch was also observed in a *syn*−*anti* conformation that distorts the DNA duplex (*54*, *55*). In this work, a comparison of ligation efficiency with different oxidized lesions provides information about the influence of purine modifications on base stacking and base pairing related to enzyme activity.

Since the redox potential of OG (0.7 V) is lower than those of the unmodified bases T (1.7 V), C (1.6 V), A (1.4 V), and G (1.3 V), it is readily oxidized by one-electron oxidants, peroxynitrite, carbonate radicals, and singlet oxygen (*56*, *57*). Two oxidation products of OG, guanidinohydantoin (Gh) and spiroiminodihydantoin (Sp), have been identified as arising from direct four-electron oxidation of G (e.g., by $^1O_2$) or further oxidation of initially formed OG (*58*−*60*) (Figure 2). Sp was recently detected in repair-deficient bacteria exposed to chromate (*61*). The levels of Gh and Sp arising from OG during in vitro oxidation of calf thymus DNA with peroxynitrite ($ONOO^-$) were 3.7 and 0.6%, respectively (*62*). Both Gh and Sp can exist as two diastereomers (*58*), and recent computational studies have revealed that the *R* and *S* stereoisomers of Sp distort the duplex by perturbing the base stacking and neighboring hydrogen binding (*63*). OG, Gh, and Sp have been studied in primer extension experiments with the Klenow fragment (KF) of *E. coli* polymerase I (*64*). Unlike OG-containing templates for which dCMP and dAMP insertion is facile, the presence of Gh or Sp in a template is inhibitory with respect to primer extension, although small amounts of dAMP and dGMP are incorporated opposite these lesions (*64*). In vivo studies in *E. coli* showed that the lesions OG and Gh were easily bypassed, and OG exhibited a weak overall mutagenesis that was largely G → T (*65*). In contrast, Gh and Sp lesions were essentially 100% mutagenic (*66*, *67*). Gh was highly specific for G → C mutations, while Sp led to both G → T and G → C mutations (*65*).

In this ligation study, both Gh and Sp were synthesized at four positions immediately surrounding the single-strand nick as comparisons to OG, OA, and OI (Figure 3); all members of this oxidized purine family have a carbonyl group at the C8 position of the original purine. To further investigate the suppressed ligation efficiencies of lesion-containing duplexes, steady-state kinetic studies (*68*) and UV melting experiments (*64*) were performed with selected lesions in the template strand. Kinetic studies with Gh·G and T·G base pairs at the 5′ end of primer 1 were also studied to test our hypothesis that Gh mimics T in a T·G wobble pair. On the basis of these results, we discuss how base stacking, hydrogen bonding, and protein−DNA interactions influence ligation efficiency.

MATERIALS AND METHODS

Oligodeoxynucleotide Synthesis and Purification. Oligodeoxynucleotides containing A, G, T, C, OG, OI, and OA were obtained either from the DNA/Peptide Core Facility (University of Utah) or synthesized on an Applied Biosystems model 392 DNA/RNA synthesizer using solid phase DNA synthesis. Sequences of the oligodeoxynucleotides that were studied are presented in Figure 3. The dOG phosphoramidite (Glen Research) was used to synthesize OG-containing oligodeoxynucleotides, which were cleaved off the column

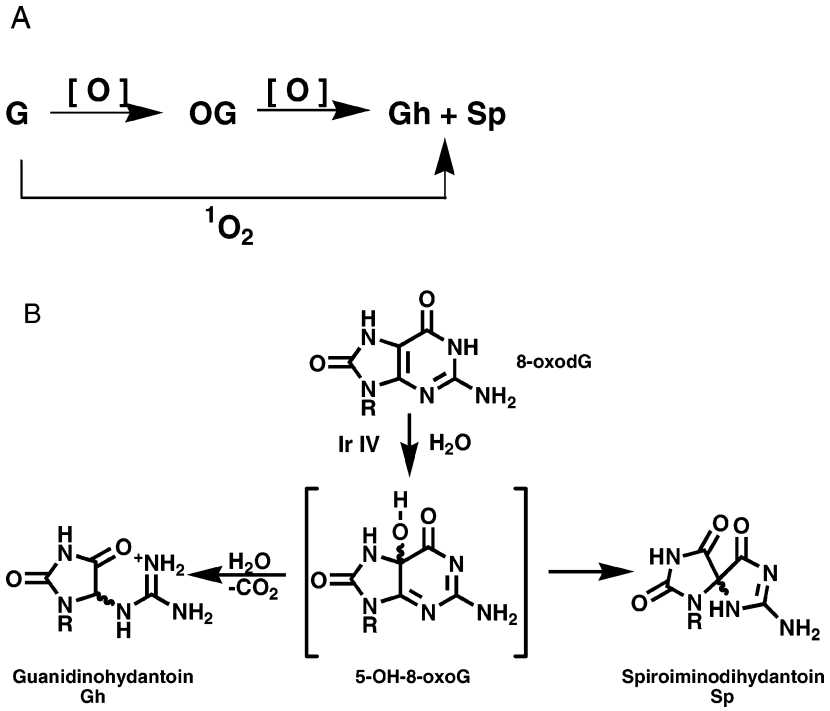

FIGURE 2: (A) Oxidation from G to Gh and Sp can occur sequentially via OG or in one step using a four-electron oxidant such as singlet oxygen. (B) Oxidation of OG with one-electron oxidants leads to Gh and Sp.

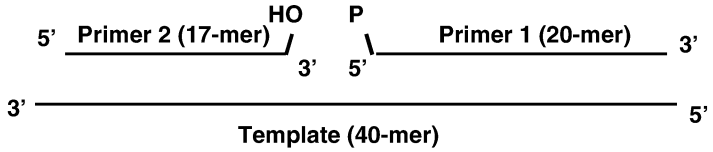

a) TemplateX/Primer1T/Primer2N (Fig. 5A): X = G, OG, Gh, Sp, OA or OI; N = C, A, T or G

5' ATT GAT GTA GCT AGC C**N**3' 5'T TAT CGG ACG CTA TCA CGT A 3'

3' TAC TAA CTA CAT CGA TCG G**X**•••A ATA GCC TGC GAT AGT GCA T 5'

b) TemplateN/Primer1T/Primer2X (Fig. 5B): X = G, OG, Gh, Sp, OA or OI; N = C, A, T or G

5' ATT GAT GTA GCT AGC C**X**3' 5'T TAT CGG ACG CTA TCA CGT A 3'

3' TAC TAA CTA CAT CGA TCG G**N**•••A ATA GCC TGC GAT AGT GCA T 5'

c) TemplateX/Primer1N/Primer2G (Fig. 5C): X = G, OG, Gh, Sp, OA or OI; N = C, A, T or G

5' ATT GAT GTA GCT AGC CG3' 5'**N** TAT CGG ACG CTA TCA CGT A 3'

3' TAC TAA CTA CAT CGA TCG GC•••**X** ATA GCC TGC GAT AGT GCA T 5'

d) TemplateN/Primer1X/Primer2G (Fig. 5D): X = G, OG, Gh, Sp, OA or OI; N = C, A, T or G

5' ATT GAT GTA GCT AGC CG3 '5'**X** TAT CGG ACG CTA TCA CGT A 3'

3' TAC TAA CTA CAT CGA TCG GC•••**N** ATA GCC TGC GAT AGT GCA T 5'

FIGURE 3: Sequences used for template−primer 1−primer 2 duplexes.

overnight in fresh 30% NH_4OH containing 0.25% β-mercaptoethanol followed by deprotection for 17 h at 55 °C. Oligodeoxynucleotides with a 3′-OG nucleotide were synthesized using a Universal Support II column (Glen Research) and cleaved using 3 mL of 2 M ammonia in methanol for 30 min at room temperature followed by deprotection for 24 h at 55 °C. The dOI phosphoramidite was synthesized by a modification of the method reported by Oka and

Greenberg (*69*), the details of which will be reported elsewhere. The dOI and dOA (Glen Research) phosphoramidites were used to synthesize OI- and OA-containing oligodeoxynucleotides, which were subsequently deprotected and cleaved with the same method as the OG-containing oligodeoxynucleotides. Purification of the oligodeoxynucleotides was accomplished using 15 or 20% denaturing polyacrylamide (19:1) gel electrophoresis (PAGE) with 6 M urea. ESI-MS analysis on a Micromass Quattro II mass spectrometer was used to verify the identity and purity of the oligodeoxynucleotide.

DNA Oxidation. OG-containing oligodeoxynucleotides were desalted twice using a G-25 column. The oligomer (12 μM) and Na_2IrCl_6 (100 μM Alfa Aesar) in a 500 μL reaction volume were used for the oxidation of OG to Gh or Sp. For the synthesis of Gh from OG, the oligodeoxynucleotides were oxidized by incubation with the oxidant for 30 min at room temperature in H_2O, whereas Sp was generated from OG by incubation for 30 min at 65 °C in 10 mM sodium phosphate (NaP_i)/100 mM NaCl buffer (pH 7.4). Oxidation reactions were quenched by addition of 4 μL of 20 mM EDTA (pH 8.5). Oxidized products were dialyzed (3500 MWCO) against water for 24−48 h to remove Na_2IrCl_6, NaPi, NaCl, and EDTA. Oligomers containing OG, Gh, or Sp lesions were purified by HPLC (Figure S1 of the Supporting Information). All other lesion-containing sequences were also subjected to HPLC purification. The purity of the oligodeoxynucleotides used for ligation was >99% (Figure S2 of the Supporting Information). ESI-MS analysis confirmed the purity of the Gh and Sp oligodeoxynucleotides.

Mass Spectrometric Analysis and HPLC Analysis. Oligodeoxynucleotides (2 nmol) in 30 μL of H_2O were combined with 10 M NH_4OAc (30 μL) for 2 h at room temperature. A 50:50 mixture of ethanol and 2-propanol (180 μL) was added, and the sample was stored for more than 2 h in dry ice, followed by centrifugation for 30 min at 4 °C. The supernatant was removed, and 1 mM NH_4OAc was added to produce a solution with a DNA concentration of 40 μM. 2-Propanol was added to yield a final concentration of 20 μM. The resulting sample was then used for ESI-MS analysis.

End Labeling of Primers and Template−Primer Annealing. Primer 1 with a native base on the 5′ end was 5′ end-labeled with T4 polynucleotide kinase (New England Biolab) and [γ-^{32}P]ATP (Amersham). Primer 1 with OG, OI, or OA on the 5′ end was first 5′ end-phosphorylated with T4 polynucleotide kinase and 1 mM nonradioactive ATP and then 3′ end-labeled with terminal transferase (New England Biolab) and [α-^{32}P]dideoxyATP (Amersham). A microspin G-25 column (Amersham Pharmacia Biotech) was used to remove unreacted [γ-^{32}P]ATP and [α-^{32}P]dideoxyATP from the radioactive DNA. Complementary oligodeoxynucleotides listed in Table 1 were annealed in water with a template: primer 1:primer 2 ratio of 2:1:1 at 90 °C for 5 min followed by slow cooling to room temperature. The final concentration of the duplex was 0.25 μM.

Ligation with T4 DNA Ligase. Ligation of the duplex was carried out with T4 DNA ligase (New England Biolabs) in 1× T4 DNA ligase buffer [50 mM Tris-HCl, 10 mM $MgCl_2$, 10 mM DTT, 1 mM ATP, and 25 μg/mL BSA (pH 7.5 and 25 °C)]. The reaction mixture included 0.125 μM duplex and 0.625 unit of T4 DNA ligase. Reaction mixtures were incubated at 25 °C for 20 min. All reactions were inactivated by incubating the mixture at 90 °C for 10 min, and then the mixtures were lyophilized to dryness. Loading buffer (8 μL of 5% bromophenol blue and 5% xylene cyanol FF in 6 M urea) was added to the sample, and a 4 μL aliquot was then taken out and loaded onto a 20% denaturing PAGE gel with 6 M urea. Gels were then analyzed by storage phosphor autoradiography on a Typhoon instrument and quantified with ImageQuant. Data presented are the averages of three or four independent experiments.

Table 1: Steady-State Kinetic Parameters of Ligation with Lesions on the 3′ End of the Nick (Figure 5B)

	K_m (μM)	k_{cat} (min^{-1})	k_{cat}/K_m (min^{-1} μM^{-1})	T_m (°C)
G•C	0.064 ± 0.008	0.51 ± 0.02	7.99	58 ± 1
OG•C	5.8 ± 1.3	1.15 ± 0.21	0.20	58 ± 3
OG•A	0.36 ± 0.11	0.61 ± 0.06	1.69	57 ± 1
OI•C	>10[a]			58 ± 2
OI•A	5.9 ± 2.1	0.55 ± 0.02	0.09	59 ± 4
OA•T	6.5 ± 2.7	0.69 ± 0.23	0.11	57 ± 1
Gh•A	1.2 ± 0.4	0.45 ± 0.007	0.36	58 ± 1
Gh•G	2.8 ± 0.5	0.22 ± 0.02	0.08	60 ± 1
Sp•A	4.5 ± 1.3	0.52 ± 0.11	0.11	61 ± 1
Sp•G	2.0 ± 0.5	0.08 ± 0.01	0.04	59 ± 1

[a] Estimated K_m value. The Michaelis−Menten curves for some duplexes do not reach a plateau.

Determining the Concentration of Active T4 DNA Ligase. Primer 2 containing a 3′-amino group on the 3′-terminal nucleotide was synthesized by transferring a 3′-amino-2′,3′-dideoxycytidine 5′-triphosphate (TriLink BioTechnologies) using terminal transferase. After purification by HPLC, primer 2 was annealed with primer 1 and template to form a nicked substrate containing a 5′-phosphate and a 3′-amino group with no lesion. A T4 DNA ligase burst assay was performed with a 100-fold dilution of the enzyme (400 units/μL) and 50 nM substrate. Data were fit in the burst equation to calculate the active enzyme concentration.

Steady-State Kinetics for the Overall Ligation Assay. To investigate the substrate specificity of T4 DNA ligase, ligation reactions with various DNA substrates containing lesions in the template were performed under the same conditions used for qualitative studies. Steady-state kinetics experiments were performed in a saturating concentration of ATP (1 mM) with various amounts of DNA substrates (from 7.5 nM to 2 μM) and different enzyme concentrations. The annealed duplex containing a normal G•C pair at the nick site required 6 units of T4 DNA ligase. Ligation with an OG•A base pair utilized 20 units, while duplexes containing Gh and Sp required 40 units of enzyme. Kinetic studies with OI- and OA-containing duplexes were performed with 80 units of enzyme. Various amounts of enzyme (6−80 units) and different reaction times (1−3 min) were used to ensure single-turnover conditions (*70*). Reaction samples were quenched with loading buffer and applied to a 20% denaturing PAGE gel. Ligation products were visualized with a Typhoon instrument and quantified with ImageQuant. K_m and k_{cat} values were calculated with Grafit 5. Kinetic studies of Gh•G and T•G base pairs were compared using the same method.

UV Melting Studies. DNA duplexes with lesions in the template were used for UV melting studies. T_m values for each duplex were measured with a Beckman DU7400 UV−

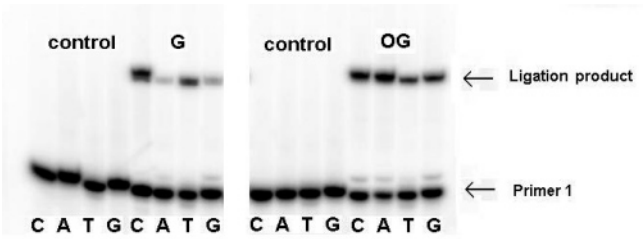

FIGURE 4: Ligation with lesions in the template opposite the 3′ end of the nick. G-, OG-, Gh-, and Sp-containing oligomers were each base paired with C, A, T, and G in the opposite strand. Lanes without ligation products were control studies with no enzyme added. Sequences are given in Figure 3a.

vis spectrophotometer. Methods were the same as those described by Kornyushyna et al. (*64*).

RESULTS

Oligodeoxynucleotides were synthesized with each of six lesions incorporated at one of four positions, on either the 3′ terminus or the 5′ terminus of the nick, or in the template opposite the two sites. For each position, a C, A, T, or G nucleotide was synthesized in the opposite strand, bringing the total number of different nicked duplexes that were studied to 96. Oligodeoxynucleotides containing lesions on the 3′ end of the nick were synthesized with a Universal Support II column using an input sequence with one extra nucleotide on the 3′ end. OG-, OA-, and OI-containing oligodeoxynucleotides were synthesized using the corresponding phosphoramidites. Gh- and Sp-containing oligodeoxynucleotides were prepared from OG-containing oligodeoxynucleotides by oxidation. All synthetic oligodeoxynucleotides were purified by PAGE, and their purity was checked by ESI-MS. After further purification by HPLC, the purities of oligodeoxynucleotides were greater than 99%. The diastereomers of Gh were used in the experiments as a mixture because they slowly interconvert and cannot be isolated (*71*). Sp diastereomers were also used as a mixture because they behaved similarly in an in vivo lesion bypass assay (*72*). Primer 1 was labeled using [γ-^{32}P]ATP and T4 polynucleotide kinase and then annealed with the template strand and primer 2. Bacteriophage T4 DNA ligase was added, and the product was visualized and quantified by PAGE storage phosphor autoradiography.

Ligation with OG, OI, and OA Lesions. The extent of ligation by T4 DNA ligase of oligodeoxynucleotides containing mismatches and lesions was first investigated using template X with primer 1T and primer 2N (X = G or OG; N = C, A, T, or G) (Figure 3). Template strands were annealed with the appropriate primers and ligated with T4 DNA ligase at 25 °C for 20 min. The same reaction system without enzyme was used as a control. The G·C Watson−Crick base pair, in which C occupies the 3′ side of the nick, had the highest percent ligation of ∼77%, whereas 47% of the mismatched G·T base pair was ligated (Figures 4 and 5A). G·A and G·G mismatches were barely ligated with levels of <3%. For base pairs containing OG, both OG·C and OG·A ligated to relatively large extents at ∼49 and ∼63%, respectively. The positioning of OG opposite T or G resulted in low ligation efficiencies (Figures 4 and 5A).

To gain a greater understanding of the structural features influencing helical integrity and enzyme activity, we examined the ligation with OI and OA in place of OG. Figure 5A shows the extent of ligation of substrates containing OI and OA in the template opposite the 3′ end of the nick, with OG used as a comparison. OI led to a high level of ligation when it was base paired with C and A (∼43 and ∼61%, respectively), which is similar to those of OG·C and OG·A substrates (49 and 63%, respectively). OI·T was moderately ligated at ∼27%, while the level of ligation of OI·G was less than 2%. As expected, OA behaved very unlike OG. Its base pair with a T-containing oligomer exhibited a relatively high degree of ligation (∼60%), since it is analogous to an A·T Watson−Crick base pair. Other bases opposite OA led to very low levels of ligation (≤8%).

Quantitative analysis of lesions located on the 3′ end of the nick is presented in Figure 5B. G·C, G·T, and OG·A base pairs were well ligated to an extent of approximately 70%. Other base mismatches containing the OG lesion were very poorly ligated (≤3%). When OI and OA are on the 3′ end of a nick, the difference between the two nucleotide analogues becomes obvious. The only base pair that ligated well was the OI·A base pair (∼60%), which is similar to the OG·A base pair. In the case of OA, none of the base pairs were tolerated by T4 DNA ligase (≤8%). Lesions, except for OG·A and OI·A base pairs, on the 3′ end essentially shut down the ligation activity of T4 DNA ligase, and apparently none of the 8-oxopurines is tolerated in a standard *anti* conformation.

Ligation of oligomers containing lesions at the position opposite the 5′ end of the nick in the template strand is revealed in Figure 5C. T4 DNA ligase catalyzed ligation of nearly all of the mismatches and base pairs containing the OG lesion with relatively high levels varying from 55 to 87%. For the ligation with OI, all the base pairs containing OI are well-ligated (25−67%), with those of OI·A and OI·C base pairs higher than 50%. Surprisingly, when OA was paired with C and G, the ligation efficiency was ∼22 and ∼15%, respectively. OA·A and OA·T base pair efficiencies were both lower than 4%. Overall, OA-containing oligomers do not form good substrates at this position, although OG and OI generally do so irrespective of the base opposite.

Figure 5D shows the extent of ligation when the lesion is on the 5′ end of the nick. Like other positions, G·C base pairs had the highest ligation efficiency of ∼82%. The G·T mismatch, as for other positions, was ligated best (∼62%) among all the other noncanonical base pairs. All the nucleotides base paired with OG on the 5′ end are ligated readily from 28 to 65%. Base pairs containing OI showed ligation patterns similar to those of OG base pairs. The ligation efficiencies were high, from 60 to 70%, except for that for OI·G (∼32%). OA base pairs were also ligated well, and the OA·T base pair had the highest efficiency among them (∼74%). Other OA base pairs displayed ligation efficiencies to the range of 30−40%.

Ligation with Gh and Sp Lesions. Established procedures were used to generate the Gh and Sp lesions as diastereomeric mixtures. Gh diastereomers rapidly interconvert and cannot be purified separately (*71*, *73*); Sp diastereomers are stable, but their activities with other enzymes have often been similar (*64*, *72*). For hydantoin lesions in the template opposite the 3′ end of the nick, Gh·A and Gh·G lesions were moderately ligated at ∼35 and ∼19%, respectively, while only ∼7% of Sp·A was ligated by T4 DNA ligase. Other

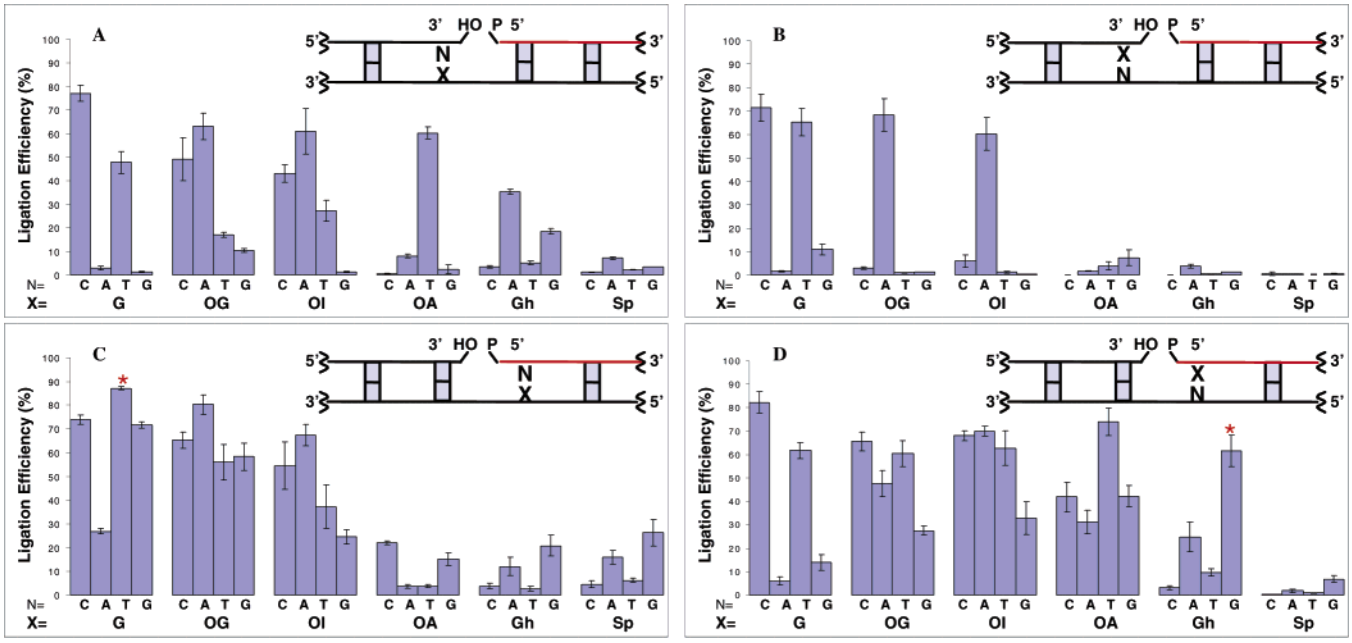

FIGURE 5: Ligation efficiencies of oligodeoxynucleotides containing OG, OI, OA, Gh, or Sp lesions (X) around the nick (X = lesion; N = C, A, T, or G): (A) lesions in the template opposite the 3′ end of the nick, (B) lesions on the 3′ end of the nick, (C) lesions in the template opposite the 5′ end of the nick, and (D) lesions on the 5′ end of the nick. DNA sequences used for panels A−D are indicated in panels a−d of Figure 3, respectively. Primer 1 (colored red) was 5′ end-labeled for PAGE analysis. Asterisks (C and D) indicate a comparison of 5′-T·G and 5′-Gh·G, both of which are ligated with high efficiency.

duplexes with Gh and Sp in the template had extremely low ligation efficiencies (≤5%) (Figure 5A).

Quantitative analysis of lesions on the 3′ end of the nick is presented in Figure 5B. All the base pairs containing Gh and Sp lesions had very low ligation efficiencies (≤3%). Gh and Sp are very poor substrates in this position, and T4 DNA ligase is very sensitive to the proper base pairing on the 3′ end of the nick.

Ligation efficiencies of lesions at the position opposite the 5′ end of the nick in the template strand are revealed in Figure 5C. Duplex DNA containing Gh and Sp base pairs had efficiencies relatively lower than those of OG base pairs. Gh·G and Sp·G were the most effectively ligated at ∼20 and ∼26%, respectively. Gh·A and Sp·A were also ligated to some extent (12 and 16%). The duplexes containing base pairs of Gh and Sp with C or T were not good substrates for ligation (≤6%).

Figure 5D shows the extent of ligation when the hydantoin lesion is on the 5′ end of the nick. Here the difference between Gh and Sp is highlighted because certain Gh-containing substrates ligated well, but none of the Sp duplexes were good substrates. The Gh·G base pair had a high ligation efficiency of ∼62%, and the Gh·A base pair was moderately ligated (∼25%). Duplexes containing Gh·C, Gh·T, and Sp lesions were barely ligated (≤10%), and although the Gh substrates were competent for being adenylated (see Figure S3C of the Supporting Information), their adenylated intermediates were not able to complete the ligation process. In a related experiment, the Sp·G base pair was only slightly ligated (∼7%), and little adenylation was observed for any Sp·N base pair. Since Gh and Sp lesions, when positioned on the 5′ end of the oligodeoxynucleotides, enhance the exonuclease activity of T4 polynucleotide kinase, degradation was observed for oligodeoxynucleotides with Gh and Sp at that position. To verify if oligodeoxynucleotides containing 5′-phosphorylated Gh and Sp lesions are efficiently ligated, experiments were carried out with 3′ end-labeled primer 1, and the results yielded similar ligation abilities (see the Supporting Information).

Concentration of Active T4 DNA Ligase. To pursue kinetic studies and obtain accurate k_{cat}/K_m data, we performed experiments to determine the concentration of active T4 DNA ligase following a protocol developed by Tsai and co-workers (*44*). The enzyme was precharged to form an enzyme−AMP intermediate by incubating a nicked DNA substrate containing a 5′-phosphate and a 3′-amino group at the nick site. The adenylation of the 5′-phosphate resulted in a rapid single turnover followed by a slow steady-state phase. Data were fit to a burst equation in which the burst amplitude corresponds to the concentration of active enzyme, determined to be 3.11 ± 0.06 μM.

Steady-State Kinetics and UV Melting Experiments. Steady-state kinetic studies using T4 DNA ligase to seal a nick were carried out with duplexes bearing lesions in the template opposite the 3′ end of the nick. An overall ligation assay was performed at a fixed and saturating concentration of ATP (1 mM), while the concentration of another substrate, the DNA duplex, was varied (from 7.5 nM to 2 μM). The values of K_m, k_{cat}, and k_{cat}/K_m were calculated for each lesion (Table 1). The relative catalytic efficiency of the G·C base pair was 4-fold higher than that of the OG·A base pair. The ligation of the OG·C base pair demonstrated an efficiency similar to those of the OI- and OA-containing duplexes, which is an ∼70-fold difference compared to that of the analogous G·C substrate. The substrates bearing further oxidized OG lesions yielded 66−180-fold lower efficiencies than G·C substrates except Gh·A, the efficiency of which is only ∼20-fold lower. G·C had the lowest K_m value at 0.064 μM; the K_m of OG·A is 5-fold higher than that of G·C, while still fairly low when compared with those of other

Table 2: Steady-State Kinetic Parameters of Ligation with Gh·G and T·G on the 5′ End of the Nick

	K_m (μM)	k_{cat} (min^{-1})	k_{cat}/K_m (min^{-1} μM^{-1})
Gh·G	1.5 ± 0.1	0.45 ± 0.02	0.31
T·G	0.055 ± 0.11	0.15 ± 0.001	0.28

lesions. Duplexes containing Gh and Sp lesions yielded K_m values much higher than that of G·C by ~18−70-fold. The Michaelis−Menten curves for OI- and OA-containing duplexes did not reach plateaus, so the K_m values were estimated to be >5 μM for these DNA substrates. k_{cat} values were similar for all the duplexes.

UV melting experiments were conducted with all the duplexes used in the kinetic studies. The 40-mer template-containing lesions were annealed with a 20-mer primer and a 17-mer primer. Most of the duplexes had T_m values around 58 °C (Table 1). Within experimental error, the T_m data showed little difference among various DNA duplexes.

Gh·G and T·G Comparison. Steady-state kinetics were studied with T or Gh on the 5′ end of primer 1 with G in the template opposite (asterisks in Figure 5, panels C and D). The ligation efficiencies for Gh·G and T·G base pairs were similar with k_{cat}/K_m values of 0.31 and 0.28 min^{-1} μM^{-1}, respectively (Table 2), although the individual k_{cat} and K_m values were quite different with Gh·G displaying weaker binding but a compensatingly higher k_{cat}. Among the 32 different orientations of hydantoin lesion base pairs (Gh·N or Sp·N), Gh·G with the Gh lesion at the 5′ end of primer 1 (asterisk in Figure 5D) exhibited the highest ligation efficiency.

DISCUSSION

In this study, we investigated the influence of the guanine oxidation product 8-oxo-7,8-dihydroguanine (OG) and the related oxidized purines, 8-oxo-7,8-dihydroadenine (OA) and 8-oxo-7,8-dihydrohypoxanthine (OI), on the ligation reaction catalyzed by bacteriophage T4 DNA ligase. Since guanosine has a lower redox potential than A, C, or T, it is the most subject to oxidation by reactive oxygen species, leading to formation of OG in, for example, the template strand of DNA. Numerous studies have established that dCTP and dATP are inserted opposite OG during replication and repair. Although misinserted dATP opposite template OG can be excised by the action of MutY in *E. coli* or hMYH in humans, a preliminary level of proofreading by inhibition of ligation of OG·A mispairs would also aid in maintaining fidelity. In contrast, previous studies have shown that duplexes containing a 3′-terminal A at the nick site opposite OG in the template are easily ligated. For example, human ligases I and III are able to join OG·A more efficiently than OG·C when OG is in the template opposite the 3′ end of the nick (Figure 5A) (*23*). The opposite base pair orientation is also biologically relevant if the dOGTP lesion is present in the nucleotide pool and is inserted opposite C or A during DNA replication (*74*, *75*). This would also require ligase to seal the nick next to a lesion, in this case at the 3′ side of OG as in Figure 5B. It is also worthwhile to study the other two positions around the nick in which lesions occupy the site at the 5′ end of the nick or the position in the template opposite the 5′ end of the nick to give a complete understanding of how the lesions in different positions could influence the ligation reaction. Although lesions at these positions near a nick (Figure 5C,D) are less likely to occur, they could be relevant to the repair of tandem lesions. We therefore designed DNA duplexes that contained lesion base pairs or mismatches at four positions surrounding the nick leading to the sequences shown in Figure 3.

Possible base pair orientations (Figure 6) for OG include the Watson−Crick base pair with C in an *anti*−*anti* conformation, although the oxygen at C8 of the purine could have detrimental interactions with the sugar−phosphate backbone. A conformational change of OG to a *syn* orientation results in a Hoogsteen base pair with an *anti* A. OI lacks the amino group at position 2 but retains the same ability to pair with C or A (*69*). Although OI is not a biologically significant lesion, it allows us to further probe the steric requirements of *syn* and *anti* 8-oxopurines in positions around the nick site. In contrast, OA has been reported to induce mutations both in vitro and in vivo (*53*). Although thymine is preferentially incorporated opposite 8-oxoA by KF and *Taq* pol, pol α and β can also incorporate dGMP as well as dCMP opposite 8-oxoA (*76*, *77*). Figure 6 shows the structure in which OA is paired with T in an *anti*−*anti* conformation. Additionally, OA can also base pair with C in a *syn*−*anti* conformation by adopting a Hoogsteen wobble structure (*55*). Thus, many possible base mismatches could be accommodated in duplex DNA if DNA ligase is able to seal nicks surrounding these lesions.

The results obtained in this study lead to several important conclusions. Consistent with other studies, the ligation reactions showed that T4 DNA ligase is more affected by a 3′-terminal lesion or mismatch at the nick site (Figure 5B) and, to a lesser extent, to lesions in the template opposite the 3′ end of the nick (Figure 5A). The data shown in the OG panel of Figure 5A are similar to the results of Moriya and co-workers who studied human DNA ligases I and III and found more efficient ligation with A at the 3′ terminus opposite OG (*23*). In the study presented here, substrates containing a 3′-terminal A were preferred versus those containing a 3′-terminal C, although the differences were not large. However, a dramatic difference was seen when the positions were reversed, i.e., when the 8-oxopurine was present at the 3′ terminus next to the nick (Figure 5B). These substrates were either very efficiently ligated (>65%) or not ligated at all (<5%). For example, the OG·A base-paired substrate was very efficiently ligated, while the OG·C substrate was not. Similarly, the OI·A substrate was efficiently ligated, while the OI·C base pair was not a substrate. These results suggest that the active site of the enzyme cannot accommodate the oxo group protruding at C8 of the purine and must flip to a *syn* conformation. Additional evidence is seen in the fact that OA at the 3′ end of the nick is not a substrate no matter what base is opposite in the template (Figure 5B), although it is efficiently ligated when it resides in the template and has T at the 3′ nick site (Figure 5A). Thus, data for the 8-oxopurines show that only the *syn* orientation is allowed when the purine is at the 3′ end of the nick, but additionally, a reasonably stable *syn*−*anti* base pair is also a requirement for ligation since OA was not well ligated with any base opposite. In contrast, 8-oxopurines can adopt either the *syn* or *anti* conformation when they reside in the template opposite the 3′ end of the nick.

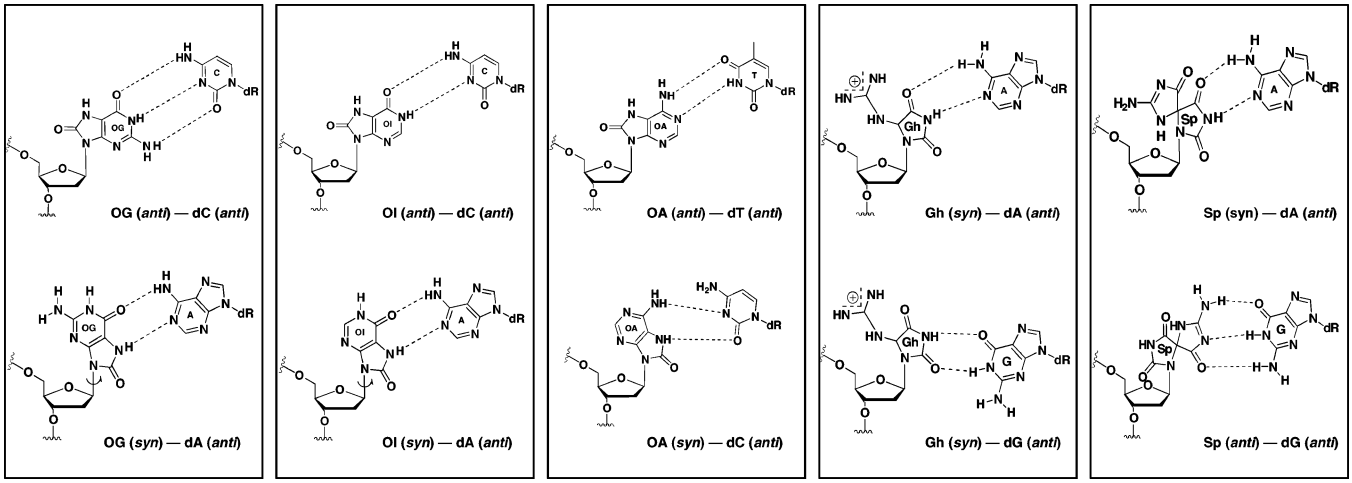

FIGURE 6: Base pairing of OG, OI, OA, Gh, and Sp. OG can base pair with C in an *anti*−*anti* conformation and with A in a *syn*−*anti* conformation. OI can form a similar base pair with the same conformation as OG. OA can form only an *anti*−*anti* base pair with T. Gh is proposed to base pair with A and G in a *syn*−*anti* conformation. Sp is proposed to base pair with A or G in a *syn*−*anti* conformation or potentially with G in an *anti*−*anti* conformation (shown).

These preferences in ligation are consistent with nucleotide insertion and primer extension studies in which dAMP and dCMP were found to be incorporated opposite OG and OI (*69*) and dTMP was incorporated opposite OA (*64*, *77*). Lesions in the template are relatively dangerous to cells since they may not be readily removed by short-patch base excision repair (BER) (*23*). Also, the 3′ → 5′ exonuclease activity of human apurinic endonuclease 1 (APE1) does not discriminate OG·A from OG·C (*41*). Furthermore, human DNA ligases I and III ligated OG·A more efficiently than OG·C when OG was located in the template (analogous to Figure 5A) (*23*).

A previous study showed that the 3′-terminal OG·C base pair inhibits ligation by DNA ligase I or DNA ligase IIIα (*78*); our results suggest that the 3′ end OG·A base pair is much more efficiently ligated. This is also consistent with ligation data reported by Wallace and co-workers, although we did not observe significant ligation with substrates containing an OA·T base pair (*50*). OA could also form an OA·C base pair with a *syn*−*anti* conformation; however, it is believed to be a Hoogsteen wobble base pair that distorts the DNA duplex and is unsuitable for normal base pairing in A or B forms of DNA (*55*).

One of the major differences between an *anti* and a *syn* conformation of OG (or OI) is that the oxo group at C8 is oriented in a different groove. This hydrogen bond acceptor is extended in the major groove in an *anti* conformation while flipped to the minor groove in a *syn* conformation. An explanation for their difference in reactivity is that the ligase may stabilize the 3′-terminal hydrogen bond with an acceptor in the minor groove that would position it for "in line" attack at the 5′-phosphate. This hydrogen bond acceptor would normally be O^2 of a pyrimidine in a T·A (or C·G) base pair, but the 8-oxo group of OG or OI could play this role in the OG·A or OI·A mispairs. An alternative explanation is that both *anti* conformations of OG and OI have a carbonyl group in the major groove that may clash with the protein. It has been found that DNA ligase fidelity is ensured by interrogation of minor groove contacts (*79*). A pyrimidine shape analogue, difluorotoluene (DFT), was used to replace thymine, and although DFT paired with adenine approximates Watson−Crick geometry, a minor groove hydrogen bond acceptor is lost and the ligation was inhibited (*79*). This result may help explain why T4 DNA ligase favors OG and OI in the *syn* conformation, although the possibility of steric interaction with the major groove is not ruled out. Overall, the 3′ end of the nick is the most important position in the ligation process, since it increases the fidelity of DNA ligase by its strict requirement for in line attack on the 5′-phosphate (*28*, *41*).

Lesions occurring on the 5′ terminus and in the template opposite the 5′ end of the nick were also studied, although their existence in vivo is considered minor. T4 DNA ligase does not differentiate mismatches at these positions and efficiently ligates all the mismatches containing OG, OI, and OA (Figure 5D). In the position opposite the 5′ end of the nick, OA·C and OA·G mismatches were weakly ligated, while ligation of OA·A and OA·T mismatches was virtually nonexistent (Figure 5C). This differs from OG and OI, which also suggests that OA behaves differently with an amino group at position 6 and its poor ability to flip over to form a *syn* conformation. Overall, the 5′ terminus of the nick contributes less to the fidelity of ligase than the 3′ end of the nick.

Although a crystal structure of T4 DNA ligase has not been published, it is reasonable to assume that the AMP covalently bound to the 5′-phosphate is stabilized by a number of amino acids in the adenylation domain of ligase in a comparison of active site amino acids of T4 DNA ligase with human DNA ligase I (*27*). It is stabilized and ready to be attacked by the 3′-OH group despite the poor base pairing resulting from the presence of OG, OI, and OA. The 3′ end of the nick may have less contact with the enzyme when a lesion is present, making it sensitive to the base pair stability and increasing the enzyme's fidelity. The published crystal structure of human DNA ligase I in association with an adenylated DNA substrate demonstrated that the 5′-phosphorylated end is positioned in the active site, and the 5′ AMP interacts extensively with Glu621, Arg573, and Lys568 (*27*). These interactions lower the energetic requirement of the base pairing at the 5′ end of the nick, while the 3′-OH group has few interactions with the enzyme and therefore is more dependent on the proper base pair chemistry in helping the OH group attack the 5′-phosphate group (*27*).

Once OG forms in the DNA duplex, it has the potential to be oxidized to the secondary oxidation products Gh and Sp; the latter has been detected in repair-compromised cells exposed to chromate (*80*). In primer extension experiments, dATP and dGTP are inserted opposite Gh and Sp, which suggests a reason that these oxidative lesions are highly mutagenic to *E. coli* (*64*, *72*, *81*, *82*). Ligation with Gh and Sp in the four positions around the nick was also studied (Figure 5). Except for the 3′ end of the nick, Gh and Sp in other positions were able to be ligated when placed opposite A and G, which conforms to the preference observed in primer extension experiments. Gh and Sp on the 3′ end of the nick totally blocked the ligation, likely because of poor base pairing with nucleotides and disruption of the helical structure. Although Gh and Sp might pair with A and G, the ligation efficiencies of Gh- and Sp-containing base pairs were found to be very low (mostly <30%).

To further investigate the ligation inhibition of lesion-containing duplex DNA, we measured the kinetic parameters k_{cat} and K_m for a representative series of base pair combinations and examined thermal stability via UV melting experiments. For the DNA duplexes used in our ligation study, including Watson−Crick and Hoogsten base pairs and base mismatches, UV melting experiments showed very similar T_m data, providing evidence that one unmatched base pair at the nick site did not destabilize the overall 37-mer DNA duplex to a large extent, although local fraying could be occurring.

Steady-state kinetic studies were carried out with template X, primer 1T, and primer 2N (Figure 3). We found that k_{cat} values for all the duplexes were similar, which suggested T4 DNA ligase converts the same amount of substrates to product per second despite the presence of lesions. The main factor influencing ligation efficiency is K_m. The OG·A-containing nicked duplex had a K_m value 5-fold higher than that of its G·C base counterpart. OG·C, OI·C, OI·A, and OA·T had much higher K_m values (>90-fold higher than that of G·C), while Gh·A, Gh·G, and Sp·G had intermediate K_m values (20−40-fold higher than that of G·C). K_m values measure the binding ability between the enzyme and substrate, and since the k_{cat} values were similar for each lesion-containing duplex, we suggest that oxidized purine lesions inhibit the binding of the enzyme to these DNA substrates, lowering the ligation efficiencies. The altered hydrogen bonding of an unmatched base pair distorts the duplex, which influences the formation of the enzyme−substrate complex. The hydrogen bonding of base pairs has a minor influence on the chemical reaction to form products. Consistent with the structures of lesion base pairs (Figure 6), T4 DNA ligase may favor a hydrogen acceptor in the minor groove or potentially a hydrogen donor in the major groove. OG·A, Gh·A, Gh·G, and Sp·G are all proposed to have *syn*−*anti* conformations in the duplex, which all have an oxo group in the minor groove and an amino group in the major groove. Their relatively low K_m values suggested that they are good substrates for T4 DNA ligase. OI·A also adopts a *syn*−*anti* conformation.

Gh and Sp make weak base pairs with normal nucleotides due to the presence of an sp^3-hybridized carbon that prevents normal base stacking and must lead to helix distortion. However, Gh is apparently able to pair somewhat with A and G compared to other bases. We propose that Gh adopts the *syn* orientation when paired with A and G, in which the hydantoin ring is positioned to mimic a T in hydrogen bonding. This hypothesis easily explains the high ligation efficiency of the substrates containing the Gh·A mismatch as well as the Gh·G mismatch, which may mimic the T·G wobble pair. For a T·G wobble pair (or U·G wobble pair in RNA), the pyrimidine is shifted toward the major groove to provide an appropriate hydrogen bonding partner with G. The same orientation in a Gh·G pair would shift the nonplanar Gh residue toward the major groove creating more space for the sp^3 carbon while providing hydrogen bond complementarity with G. The observation of similarly high ligation efficiencies with Gh·G and T·G pairs at the 5′ terminus is an interesting result that may support this hypothesis (compare the asterisks in panels C and D of Figure 5).

Our current data suggest that, except for the OG·A mismatch, OG, OA, OI, Gh, and Sp are poor substrates for ligation especially when they are located at the 3′ end of the oligomer to be ligated. Discrimination against ligation of a 3′-terminal lesion provides a means of proofreading of single-nucleotide misincorporation during BER. Suppression of DNA ligation under oxidative stress is one possible mechanism for reducing the level of spontaneous mutation. However, oxidative lesions occurring in the template are still potential threats to the cell. Whenever C and A are inserted opposite OG or A and G are inserted opposite Gh, these mismatches will be efficiently ligated, potentially resulting in cellular mutation.

SUPPORTING INFORMATION AVAILABLE

HPLC analysis of crude and purified OG-, Sp-, and Gh-containing oligomers, PAGE analysis of OI- and OA-containing oligomers, and comparison of ligation of oligomers with lesions on the 5′ terminus of primer 1. This material is available free of charge via the Internet at http://pubs.acs.org.

REFERENCES

1. Shigenaga, M. K., Gimeno, C. J., and Ames, B. N. (1989) Urinary 8-hydroxy-2′-deoxyguanosine as a biological marker of in vivo oxidative DNA damage, *Proc. Natl. Acad. Sci. U.S.A. 86*, 9697−9701.
2. Finkel, T., and Holbrook, N. J. (2000) Oxidants, oxidative stress and the biology of ageing, *Nature 408*, 239−247.
3. Feig, D. I., and Loeb, L. A. (1994) Oxygen radical induced mutagenesis is DNA polymerase specific, *J. Mol. Biol. 235*, 33−41.
4. Wiseman, H., and Halliwell, B. (1996) Damage to DNA by reactive oxygen and nitrogen species: Role in inflammatory disease and progression to cancer, *Biochem. J. 313*, 17−29.
5. Steenken, S., and Jovanovic, S. J. (1997) How easily oxidizable is DNA? One-electron reduction potentials of adenosine and guanosine radicals in aqueous solution, *J. Am. Chem. Soc. 119*, 617−618.
6. Shigenaga, M. K., Aboujaoude, E. N., Chen, Q., and Ames, B. N. (1994) Assays of oxidative DNA damage biomarkers 8-oxo-2′-deoxyguanosine and 8-oxo-guanine in nuclear DNA and biological fluids by high-performance liquid chromatography with electrochemical detection, *Methods Enzymol. 234*, 16−33.
7. Cadet, J., Bellon, S., Berger, M., Bourdat, A. G., Douki, T., Duarte, V., Frelon, S., Gasparutto, D., Muller, E., Ravanat, J. L., and Sauvaigo, S. (2002) Recent aspects of oxidative DNA damage: Guanine lesions, measurement and substrate specificity of DNA repair glycosylases, *Biol. Chem. 383*, 933−943.

8. Neeley, W. L., and Essigmann, J. M. (2006) Mechanisms of formation, genotoxicity, and mutation of guanine oxidation products, *Chem. Res. Toxicol. 19*, 491−505.
9. Lindahl, T. (1993) Instability and decay of the primary structure of DNA, *Nature 362*, 709−715.
10. Greenblatt, M. S., Bennett, S. E., Hollstein, M., and Harris, C. C. (1994) Mutations in the p53 tumor suppressor gene: Clues to cancer etiology and molecular pathogenesis, *Cancer Res. 54*, 4855−4878.
11. David, S. S., and Williams, S. D. (1998) Chemistry of glycosylases and endonucleases involved in base-excision repair, *Chem. Rev. 98*, 1221−1261.
12. Friedberg, E., Walker, G. C., and Seide, W. (1995) *DNA Repair and Mutagenesis*, ASM Press, Washington, DC.
13. Hsu, G. W., Ober, M., Carell, T., and Beese, L. S. (2004) Error-prone replication of oxidatively damaged DNA by a high-fidelity DNA polymerase, *Nature 431*, 217−221.
14. Lomax, M. E., Cunniffe, S., and O'Neill, P. (2004) Efficiency of repair of an abasic site within DNA clustered damage sites by mammalian cell nuclear extracts, *Biochemistry 43*, 11017−11026.
15. David-Cordonnier, M.-H., Boiteux, S., and O'Neill, P. (2001) Excision of 8-oxoguanine within clustered damage by the yeast OGG1 protein, *Nucleic Acids Res. 29*, 1107−1113.
16. Showalter, A. K., Lamarche, B. J., Bakhtina, M., Su, M. I., Tang, K. H., and Tsai, M. D. (2006) Mechanistic comparison of high-fidelity and error-prone DNA polymerases and ligases Involved in DNA repair, *Chem. Rev. 106*, 340−360.
17. Tomkinson, A. E., Vijayakumar, S., Pascal, J. M., and Ellenberger, T. (2006) DNA ligases: Structure, reaction mechanism, and function, *Chem. Rev. 106*, 687−699.
18. Slupphaug, G., Mol, C. D., Kavli, B., Arvai, A. S., Krokan, H. E., and Tainer, J. A. (1996) A nucleotide-flipping mechanism from the structure of human uracil-DNA glycosylase bound to DNA, *Nature 384*, 87−92.
19. Braves, R. J., Felzenszwalb, I., Laval, J., and O'Connor, T. (1992) Excision of 5′-terminal deoxyribose phosphate from damaged DNA is catalyzed by the Fpg protein of *Escherichia coli*, *J. Biol. Chem. 267*, 14429−14435.
20. Bernards, A. S., Miller, J. K., Bao, K. K., and Wong, I. (2002) Flipping duplex DNA inside out: A double base flipping reaction mechanism by *Escherichia coli* MutY adenine glycosylase, *J. Biol. Chem. 277*, 20960−20964.
21. Fortini, P., Pascucci, B., Parlanti, E., D'Errico, M., Simonelli, V., and Dogliotti, E. (2003) The base excision repair: Mechanisms and its relevance for cancer susceptibility, *Biochimie 85*, 1053−1071.
22. Slupphaug, G., Kavli, B., and Krokan, H. E. (2003) The interacting pathways for prevention and repair of oxidative DNA damage, *Mutat. Res. 531*, 231−251.
23. Hashimoto, K., Tominaga, Y., Nakabeppu, Y., and Moriya, M. (2004) Futile short-patch DNA base excision repair of adenine: 8-Oxoguanine mispair, *Nucleic Acids Res. 32*, 5928−5934.
24. Levin, D. S., McKenna, A. E., Motycka, T. A., Matsumoto, Y., and Tomkinson, A. E. (2000) Interaction between PCNA and DNA ligase 1 is critical for joining of Okazaki fragments and long-patch base-excision repair, *Curr. Biol. 10*, 919−922.
25. Levin, D. S., Bai, W., Yao, N., O'Donnell, M., and Tomkinson, A. E. (1997) An interaction between DNA ligase and proliferating cell nuclear antigen: Implications for Okazaki fragment synthesis and joining, *Proc. Natl. Acad. Sci. U.S.A. 94*, 12863−12868.
26. Tomkinson, A. E., Lasko, D. D., Daly, G., and Lindahl, T. (1990) Mammalian DNA ligases, *J. Biol. Chem. 265*, 12611−12617.
27. Pascal, J. M., O'Brien, P. J., Tomkinson, A. E., and Ellenberger, T. (2004) Human DNA ligase I completely encircles and partially unwinds nicked DNA, *Nature 432*, 473−478.
28. Lehman, I. R. (1974) DNA ligase: Structure, mechanism, function, *Science 186*, 790−797.
29. Deugau, K. V., and Sande, J. H. (1978) T4 polynucleotide ligase catalyzed joining of short synthetic DNA, *Biochemistry 17*, 723−729.
30. Shuman, S., and Schwer, B. (1995) In vitro mutagenesis and functional expression in *Escherichia coli* of a cDNA encoding the catalytic domain of human DNA ligase I, *Nucleic Acids Res. 19*, 6093−6099.
31. Bohle, D. S., Hansert, B., Paulson, S. C., and Smith, B. D. (1994) Biomimetic synthesis of putative cytotoxin peroxynitrite, $ONOO^-$, and its characterization as a tetramethylammonium salt, *J. Am. Chem. Soc. 116*, 7423−7424.
32. Malyarchuk, S., Youngblood, R., Landry, A. M., Quillin, E., and Harrison, L. (2003) The mutation frequency of 8-oxo-7,8-dihydroguanine (8-oxodG) situated in a multiply damaged site: Comparison of a single and two closely opposed 8-oxodG in *Escherichia coli*, *DNA Repair 2*, 695−705.
33. Lomax, M. E., Cunniffe, S., and O'Neill, P. (2004) 8-oxoG retards the activity of the ligase III/XRCC1 complex during the repair of a single-strand break, when present within a clustered DNA damage site, *DNA Repair 3*, 289−299.
34. Bourdat, A.-G., Douki, T., Frelon, S., Gasparutto, D., and Cadet, J. (2000) Tandem base lesions are generated by hydroxyl radical within isolated DNA in aerated aqueous solution, *J. Am. Chem. Soc. 122*, 4549−4556.
35. Lomax, M. E., Salje, H., Cunniffe, S., and O'Neill, P. (2005) 8-Oxo A inhibits the incision of an AP site by the DNA glycosylases Fpg, Nth and the AP endonuclease HAP1, *Radiat. Res. 163*, 79−84.
36. Michaels, M. L., Cruz, C., Grollman, A. P., and Miller, J. H. (1992) Evidence that MutY and MutM combine to prevent mutations by an oxidatively damaged form of guanine in DNA, *Proc. Natl. Acad. Sci. U.S.A. 89*, 7022−7025.
37. Michaels, M. L., Tchou, J., Grollman, A. P., and Miller, J. H. (1992) A repair system for 8-oxo-7,8-dihydrodeoxyguanosine, *Biochemistry 31*, 10964−10968.
38. Seeberg, E., Eide, L., and Bjoras, M. (1995) The base excision repair pathway, *Trends Biochem. Sci. 20*, 391−397.
39. Harada, K., and Orgel, L. (1993) Unexpected substrate specificity of T4 DNA ligase revealed by in vitro selection, *Nucleic Acids Res. 21*, 2287−2291.
40. Landergren, U., Kaiser, R., Sanders, J., and Hood, L. (1988) A ligase-mediated gene detection technique, *Science 241*, 1077−1080.
41. Pritchard, C. E., and Southern, E. M. (1997) Effects of base mismatches on joining of short oligodeoxynucleotides by DNA ligases, *Nucleic Acids Res. 25*, 3403−3407.
42. Cherepanov, A., Yildirim, E., and Vries, S. (2001) Joining of short DNA oligonucleotides with base pair mismatches by T4 DNA ligase, *J. Biochem. 129*, 61−68.
43. Wu, D. Y., and Wallace, R. B. (1989) Specificity of the nick-closing activity of bacteriophage T4 DNA ligase, *Gene 76*, 245−254.
44. Lamarche, B. J., Showalter, A. K., and Tsai, M. D. (2005) An error-prone viral DNA ligase, *Biochemistry 44*, 8408−8417.
45. Husain, I., Tomkinson, A. E., Burkhart, W. A., Moyer, M. B., Ramos, W., Mackey, Z. B., Besterman, J. M., and Chen, J. (1995) Purification and characterization of DNA ligase III from bovine testes, *J. Biol. Chem. 270*, 9683−9690.
46. Tomkinson, A. E., Tappe, N. J., and Friedberg, E. C. (1992) DNA ligase I from *Saccharomyces cerevisiae*: Physical and biochemical characterization of the CDC9 gene product, *Biochemistry 31*, 11762−11771.
47. Jaruga, P., and Dizdaroglu, M. (1996) Repair of products of oxidative DNA base damage in human cells, *Nucleic Acids Res. 24*, 1389−1394.
48. Bjelland, S., and Seeberg, E. (2003) Mutagenicity, toxicity and repair of DNA base damage induced by oxidation, *Mutat. Res. 531*, 37−80.
49. Olinski, R., Zastawny, T., Budzbon, J., Skokowski, J., Zegarski, W., and Dizdaroglu, M. (1992) DNA base modifications in chromatin of human cancerous tissues, *FEBS Lett. 309*, 193−198.
50. Hatahet, Z., Purmal, A. A., and Wallace, S. S. (1993) A novel method for site specific introduction of single model oxidative DNA lesions into oligodeoxyribonucleotides, *Nucleic Acids Res. 21*, 1563−1568.
51. Cheng, X., Kelso, C., Hornak, V., Santos, C., Grollman, A. P., and Simmerling, C. (2005) Dynamic behavior of DNA base pairs containing 8-oxoguanine, *J. Am. Chem. Soc. 127*, 13906−13918.
52. Shibutani, S., Bodepudi, V., Johnson, F., and Grollman, A. P. (1993) Translesional synthesis on DNA templates containing 8-oxo-7,8-dihydrodeoxyadenosine, *Biochemistry 32*, 4615−4621.
53. Kamiya, H., Miura, H., Murata-Kamiya, N., Ishikawa, H., Sakaguchi, T., Inoue, H., Sasaki, T., Masutani, C., Hanaoka, F., Nishimura, S., and Ohtsuka, E. (1995) 8-Hydroxyadenine (7,8-dihydro-8-oxoadenine) induces misincorporation in in vitro DNA synthesis and mutations in NIH 3T3 cells, *Nucleic Acids Res. 23*, 2893−2899.
54. Barone, F., Cellai, L., Giordano, C., Sala, G. L., and Mazzei, F. (2002) Influence of an 8-oxoadenine lesion on the structural and

dynamic features of a 30-mer DNA fragment with and without a mismatch, *Int. J. Radiat. Biol. 78*, 9−16.
55. Cho, B. P., and Evans, F. E. (1991) Structure of oxidatively damaged nucleic acid adducts. 3. Tautomerism, ionization and protonation of 8-hydroxyadenosine studied by ^{15}N NMR spectroscopy, *Nucleic Acids Res. 19*, 1041−1047.
56. Yanagawa, H., Ogawa, Y., and Ueno, M. (1992) Redox ribonucleosides, *J. Biol. Chem. 267*, 13320−13326.
57. Steenken, S., Jovanovic, S. V., Bietti, M., and Bernhard, K. (2000) The trap depth (in DNA) of 8-oxo-7,8-dihydro-2′-deoxyguanosine as derived from electron-transfer equilibria in aqueous solution, *J. Am. Chem. Soc. 122*, 2372−2374.
58. Luo, W., Muller, J. G., Rachlin, E. M., and Burrows, C. J. (2000) Characterization of spiroiminodihydantoin as a product of one-electron oxidation of 8-oxo-7,8-dihydroguanosine, *Org. Lett. 2*, 613−617.
59. Niles, J. C., Wishnok, J. S., and Tannenbaum, S. R. (2001) Spiroiminodihydantoin is the major product of 8-oxo-7,8-dihydroguanosine reaction with peroxynitrite in the presence of thiols, and guanosine photooxidation by methylene blue, *Org. Lett. 3*, 763−766.
60. Adam, W., Arnold, M. A., Nau, W. M., Pischel, U., and Saha-Moeller, C. R. (2002) A comparative photomechanistic study (spin trapping, EPR spectroscopy, transient kinetics, photoproducts) of nucleoside oxidation (dG and 8-oxodG) by triplet-excited acetophenones and by the radicals generated from α-oxy-substituted derivatives through Norrish-type I cleavage, *J. Am. Chem. Soc. 124*, 3893−3904.
61. Hailer, M. K., Slade, P. G., Martin, B. D., and Sugden, K. D. (2005) Nei deficient *Escherichia coli* are sensitive to chromate and accumulate the oxidized guanine lesion spiroiminodihydantoin, *Chem. Res. Toxicol. 18*, 1378−1383.
62. Yu, H., Venkatarangan, L., Wishnok, J. S., and Tannenbaum, S. R. (2005) Quantitation of four guanine oxidation products from reaction of DNA with varying doses of peroxynitrite, *Chem. Res. Toxicol. 18*, 1849−1857.
63. Jia, L., Shafirovich, V., Shapiro, R., Geacintov, N. E., and Broyde, S. (2005) Structural and thermodynamic features of spiroiminodihydantoin damaged DNA duplexes, *Biochemistry 44*, 13342−13353.
64. Kornyushyna, O., Berges, A. M., Muller, J. G., and Burrows, C. J. (2002) In vitro nucleotide misinsertion opposite the oxidized guanosine lesions spiroiminodihydantoin and guanidinohydantoin and DNA synthesis past the lesions using *Escherichia coli* DNA polymerase I (Klenow fragment), *Biochemistry 41*, 15304−15314.
65. Henderson, P. T., Delaney, J. C., Muller, J. G., Neeley, W. L., Tannenbaum, S. R., Burrows, C. J., and Essigmann, J. M. (2003) The hydantoin lesions formed from oxidation of 7,8-dihydro-8-oxoguanine are potent sources of replication errors in vivo, *Biochemistry 42*, 9257−9262.
66. Moriya, M. (1993) Single-stranded shuttle phagemid for mutagenesis studies in mammalian cells: 8-Oxoguanine in DNA induces targeted GC → TA transversion in simian kidney cells, *Proc. Natl. Acad. Sci. U.S.A. 90*, 1122−1126.
67. Le Page, F., Margot, A., Grollman, A. P., Sarasin, A., and Gentile, A. (1995) Mutagenicity of a unique 8-oxoguanine in a human Ha-ras sequence in mammalian cells, *Carcinogenesis 16*, 2779−2784.
68. Cherepanov, A., and Vries, S. (2003) Kinetics and thermodynamics of nick sealing by T4 DNA ligase, *Eur. J. Biochem. 270*, 4315−4325.
69. Oka, N., and Greenberg, M. M. (2005) The effect of the 2-amino group of 7,8-dihydro-8-oxo-2′-deoxyguanosine on translesion synthesis and duplex stability, *Nucleic Acids Res. 33*, 1637−1643.
70. Goodman, M. F., Creighton, S., Bloom, L. B., and Petruska, J. (1993) Biochemical basis of DNA replication fidelity, *Crit. Rev. Biochem. Mol. Biol. 28*, 83−126.
71. Ye, Y., Muller, J. G., Luo, W., Mayne, C. L., Shallop, A. J., Jones, R. A., and Burrows, C. J. (2003) Formation of ^{13}C-, ^{15}N- and ^{18}O-labeled guanidinohydantoin from guanosine oxidation with singlet oxygen. Implications for structure and mechanism, *J. Am. Chem. Soc. 125*, 13926−13927.
72. Henderson, P. T., Delaney, J. C., Muller, J. G., Neeley, W. L., Tannenbaum, S. R., Burrows, C. J., and Essigmann, J. M. (2003) The hydantoin lesions formed from oxidation of 7,8-dihydro-8-oxoguanine are potent sources of replication errors in vivo, *Biochemistry 42*, 9257−9262.
73. Luo, W., Muller, J. G., Rachlin, E. M., and Burrows, C. J. (2001) Characterization of hydantoin products from one-electron oxidation of 8-oxo-7,8-dihydroguanosine in a nucleoside model, *Chem. Res. Toxicol. 14*, 927−938.
74. Maki, H., and Sekiguchi, M. (1992) MutT protein specifically hydrolyses a potent mutagenic substrate for DNA synthesis, *Nature 355*, 273−275.
75. Chmiel, N. H., Golinelli, M.-P., Francis, A. W., and David, S. S. (2001) Efficient recognition of substrates and substrate analogs by the adenine glycosylase MutY requires the C-terminal domain, *Nucleic Acids Res. 29*, 553−564.
76. Wood, M. L., Esteve, A., Morningstar, M. L., Kuziembo, G. M., and Essigman, J. M. (1992) Genetic effects of oxidative DNA damage: Comparative mutagenesis of 7,8-dihydro-8-oxoguanine and 7,8-dihydro-8-oxoadenine in *Escherichia coli*, *Nucleic Acids Res. 20*, 6023−6032.
77. Guschlbauer, W., Duplaa, A. M., Guy, A., Teoule, R., and Fazakerley, G. V. (1991) Structure and in vitro replication of DNA templates containing 7,8-dihydro-8-oxoadenine, *Nucleic Acids Res. 19*, 1753−1758.
78. Parsons, J. L., Dianova, I. I., and Dianov, G. L. (2005) APE1-dependent repair of DNA single-strand breaks containing 3′-end 8-oxoguanine, *Nucleic Acids Res. 33*, 2204−2209.
79. Liu, P., Burdzy, A., and Sowers, L. C. (2004) DNA ligases ensure fidelity by interrogating minor groove contacts, *Nucleic Acids Res. 32*, 4503−4511.
80. Hailer, M. K., Slade, P. G., Martin, B. D., and Sugden, K. D. (2005) Nei deficient *Escherichia coli* are sensitive to chromate and accumulate the oxidized guanine lesion spiroiminodihydantoin, *Chem. Res. Toxicol. 18*, 1378−1383.
81. Duarte, V., Muller, J. G., and Burrows, C. J. (1999) Insertion of dGMP and dAMP during in vitro DNA synthesis opposite an oxidized form of 7,8-dihydro-8-oxoguanine, *Nucleic Acids Res. 27*, 496−502.
82. Kornyushyna, O., and Burrows, C. J. (2003) Effect of the oxidized guanosine lesions spiroiminodihydantoin and guanidinohydantoin on proofreading by *Escherichia coli* DNA polymerase I (Klenow fragment) in different sequence contexts, *Biochemistry 42*, 13008−13018.

BI062214K